

A New Lake Classification System based on Thermal Profiles to Better Understand the Most Dominant Lake Type on Earth

Bernard Yang^{1*}, Mathew G. Wells^{1*}, Bailey C. McMeans², Hilary A. Dugan³, James A. Rusak^{4,5}, Gesa A. Weyhenmeyer⁶, Jennifer A. Brentrop^{7,8}, Allison R. Hrycik^{7,9}, Alo Laas¹⁰, Rachel M. Pilla¹¹, Jay A. Austin^{12,13}, Paul J. Blanchfield^{5,14}, Cayelan C. Carey¹⁵, Matthew M. Guzzo^{2,16}, Noah R. Lottig¹⁷, Murray D. Mackay¹⁸, Trevor A. Middel¹⁹, Don C. Pierson⁶, Junbo Wang²⁰, Joelle D. Young²¹

¹ Department of Physical and Environmental Sciences, University of Toronto Scarborough, Toronto, Ontario, Canada

² Department of Biology, University of Toronto Mississauga, Mississauga, Ontario, Canada

³ Center for Limnology, University of Wisconsin-Madison, Wisconsin, USA

⁴ Dorset Environmental Science Centre, Ontario Ministry of the Environment, Conservation, and Parks, Dorset, Ontario, Canada

⁵ Department of Biology, Queen's University, Kingston, Ontario, Canada

⁶ Department of Ecology and Genetics/Limnology, Uppsala University, Uppsala, Sweden

⁷ Rubenstein Ecosystem Science Laboratory, University of Vermont, Vermont, USA

⁸ Department of Biology and Environmental Studies, St. Olaf College, Minnesota, USA

⁹ Department of Biology, University of Vermont, Vermont, USA

¹⁰ Chair of Hydrobiology and Fishery, Institute of Agricultural and Environmental Sciences, Estonian University of Life Sciences, Tartu, Estonia

¹¹ Department of Biology, Miami University, Oxford, Ohio, USA

¹² Large Lakes Observatory, University of Minnesota Duluth, Duluth, Minnesota, USA

¹³ Department of Physics and Astronomy, University of Minnesota Duluth, Duluth, Minnesota, USA

¹⁴ Fisheries and Oceans Canada, Winnipeg, Manitoba, Canada

¹⁵ Department of Biological Sciences, Virginia Tech, Blacksburg, Virginia, USA

¹⁶ Department of Integrative Biology, University of Guelph, Guelph, Ontario, Canada

¹⁷ Center for Limnology Trout Lake Station, University of Wisconsin-Madison, Wisconsin, USA

¹⁸ Environmental Numerical Weather Prediction Research, Science and Technology Branch, Environment and Climate Change Canada, Canada

¹⁹ Harkness Laboratory of Fisheries Research, Aquatic Research and Monitoring Section, Ontario Ministry of Natural Resources, Trent University, Peterborough, Ontario, Canada

²⁰ Key Laboratory of Tibetan Environment Changes and Land Surface Processes (TEL) / Nam Co Observation and Research Station (NAMORS), Institute of Tibetan Plateau Research, Chinese Academy of Sciences, Beijing 100101, China

²¹ Ontario Ministry of the Environment, Conservation, and Parks, Toronto, Ontario, Canada

*Corresponding authors: Bernard Yang (bernie.yang@utoronto.ca), Mathew Wells

(m.wells@utoronto.ca)

Key points

- Standard classifications of dimictic lakes do not consider how variable the initial thermal stratification can be under winter lake ice

- Lakes that are shallow or windy can cool to near 0-1°C before ice forms and are weakly stratified, which we term “cryomictic”
- Deeper lakes or those with calmer winds, result in ice forming just above deeper waters of 3-4°C, which we term “cryostratified”

Author Contribution Statement: This project was initiated in a workshop at the 21st Global Lakes Ecological Observatory Network meeting in Huntsville, Ontario, Canada in 2019. The authors are listed in four groups: BY-BCM; HAD-GAW; JAB-RMP; and JAA-JDY. The first group is listed in order of contribution in writing the manuscript. The second group, listed alphabetically, includes authors who attended the workshop, and participated in the initial framing for the project, and were involved in designing the structure of the manuscript. The third group, listed alphabetically, attended the workshop and participated in the initial framing for the project. The fourth group, listed alphabetically, prepared data for the analysis and contributed feedback. The specific contributions are as follows: BY and MGW conceived the idea for the manuscript and coordinated the project. HAD, ARH, AL, RMP, GAW, MGW, and BY participated at the initial project discussion during the meeting. BY conducted the data analysis and prepared the figures. HAD, JAR, GAW, MGW, and BY designed the manuscript. BY wrote the manuscript under the supervision of MGW. BCM wrote the section on biological influences. JAA, JAB, PJB, CCC, HAD, MMG, ARH, AL, NRL, MDM, TAM, DCP, RMP, JAR, JW, MGW, BY, and JDY prepared the data for the analysis. All authors provided critical feedbacks and approved the manuscript.

Abstract

Lakes are traditionally classified based on their thermal regime and trophic status. While this classification adequately captures many lakes, it is not sufficient to understand seasonally ice-covered lakes, the most common lake type on Earth. Here, we propose an additional classification to differentiate under-ice stratification. When ice forms in smaller and deeper lakes, inverse stratification will form with a thin buoyant layer of cold water (near 0°C) below the ice, which remains above a deeper 4°C layer. In contrast, the entire water column can cool to ~0°C in larger and shallower lakes. We suggest these alternative conditions for dimictic lakes be termed “cryostratified” and “cryomictic.” We describe the inverse thermal stratification in 19 highly varying lakes and derive a model that predicts the temperature profile as a function of wind stress, area, and depth. The model opens up for a more precise prediction of lake responses to a warming climate.

Plain Language Summary

Most mid and high latitude lakes are seasonally ice-covered and have only been classified based on the thermal structure and trophic status during the open-water season in summer. However, limited temperatures observations in these ice-covered lakes suggest that there is a wide range of thermal structures over winter. We developed an analytical model to predict the average water temperature at the time of ice formation based on the strength of the surface winds, the area of

the lake, and the maximum depth of the lake. Using both the analytical model and water temperature data from 19 different lakes in North America, Europe, and Asia, we found that the time of ice formation in lakes that are large or experience strong winds were later compared to lakes that are small or experience weak winds. The larger and windier lakes are also generally colder ($0\sim 2^{\circ}\text{C}$) than smaller and calmer lakes ($2\sim 4^{\circ}\text{C}$) at the time of ice formation. This suggests that these seasonally ice-covered lakes can be subdivided into two additional classes during winter. The analytical model and the new classification have important consequences for understanding fish habitat under the ice and the potential effects of climate change on these seasonally ice-covered lakes.

Introduction

At least 50% of the lakes in the world are located at high latitudes and are seasonally ice-covered (Verpoorter et al., 2014). Therefore, it is important to understand the broad controls on thermal stratification present during winter in these ubiquitous cold monomictic and dimictic lakes at temperate and boreal regions. In both types of lakes, the water column becomes thermally stratified under lake ice in the winter. While considerable effort has been made to describe the details and drivers of summer thermal stratification in dimictic lakes (e.g., Bohrer and Schultze, 2008), most textbooks do not go much beyond saying that during winter an inverse stratification exists (e.g., Wetzel, 2001), following the original classification scheme of dimictic lakes by Lewis (1983). In the lake classification scheme given by Lewis (1983), only four examples of dimictic lakes are given, of which only 2 lakes (Lake Erken in Sweden and Lake Mendota in Wisconsin, USA) were not meromictic. It is unclear, however, to what degree these two lakes should be considered archetypes of winter conditions in *all* dimictic lakes. In particular, the strength of thermal stratification and mixing that occurs before and during ice formation remains unknown, as under-ice processes have been reported in only 2% of the peer-reviewed literature on freshwater systems (Hampton et al., 2015, 2017). Once ice onset occurs in dimictic lakes, the initial thermal stratification present during ice formation largely persists through the whole winter prior to the late-winter convection period (Bruesewitz et al. 2015; Yang et al., 2017, 2020; MacKay et al. 2017). The resulting under-ice thermal profile regulates biological activity, as both a habitat for fish (McMeans et al., 2020), plankton (Kelley, 1997, Hampton et al., 2015), and as a control on microbial processing. It also influences lake hydrodynamics, through control on internal waves, circulation and vertical mixing (Kirillin et al., 2012). Consequently, determining the drivers of under-ice thermal stratification in dimictic lakes is needed to better understand under-ice conditions as they rapidly change (Hampton et al., 2017), especially as lakes are warming under a changing climate (O'Reilly et al., 2015).

The extent of surface mixing after the water column cools to 4°C and before ice forms in the fall or early winter controls the heat distribution through the water column, and thus influences the thermal stratification at ice-on (Figure 1). The mixing dynamics are determined by the non-linear equation of state, where freshwater becomes less dense as temperature decreases below 4°C . Thus, cooling that occurs above 4°C destabilizes the water-column, whereas when the water-column cools below 4°C there is a stabilizing buoyancy flux that restratifies the water column (Farmer and Carmack, 1981). In general, lakes subjected to more intense wind mixing during late fall will have lower water column temperatures, so that wind speed prior to ice formation

should determine early winter temperature profiles (Farmer and Carmack, 1981). Using the idea of a one-dimensional Monin-Obukhov scaling, Farmer and Carmack (1981) suggested that a vertical length scale for the cold buoyant layer is $H_{FC} \sim u_*^3/B$, where u_* is the friction velocity and B is the buoyancy flux per unit area. Hence stronger winds result in a deeper cold layer before ice-on (Figure 1a,1c), whereas calmer lakes have shallower cold surface layers (Figure 1b,1d). The same balance between vertical mixing and a stable buoyancy flux applies to the summer thermocline, and a similar Monin-Obukhov scaling argument has been used by Kirillin and Shatwell (2016) to separate the summer stratification of 378 lakes into polymictic or stratified dimictic systems.

The physics of inverse stratification prior to formation of ice cover is analogous to the widely studied process of thermocline formation in early summer in dimictic lakes. For instance, the depth of a dimictic lake's thermocline can also be related to the magnitude of wind-driven mixing and the lake's geometry. Gorham and Boyce (1989) used a two-dimensional argument based on the Wedderburn number to show that the depth of the late summer thermocline scaled as

$$H_{GB} \sim \bar{u}_* \sqrt{L/g'} \quad (1)$$

where \bar{u}_* is the friction velocity averaged over the summer stratified period, L the fetch and g' the reduced gravity across the thermocline, defined as $g' = g \Delta\rho/\rho_o$, where g is the gravitational acceleration, $\Delta\rho$ is the density difference across the thermocline, and ρ_o is the average density of the water column. In contrast to the one-dimensional Monin-Obukhov scaling used by Farmer and Carmack (1981) and Kirillin and Shatwell (2016), this scaling explicitly includes the effects of the lake geometry, namely the fetch of the lake. Gorham and Boyce (1989) found a good agreement with their prediction when looking at end-of-summer thermocline depths H in 150 lakes. Fee et al. (1996) found that H during midsummer had a positive correlation with $A^{\frac{1}{4}}$, where A is the surface area of the lake. If the lake is circular, then $A^{\frac{1}{4}} \sim L^{\frac{1}{2}}$. For a fixed wind speed, this is the same scaling relationship as $H_{GB} \sim L^{\frac{1}{2}}$ obtained by Gorham and Boyce (1989). Both the one and two-dimensional arguments suggest that with more wind, the thermocline during the formation of stratification in a dimictic lake becomes deeper, a result that applies to both early summer and early winter. However, this scaling has never been applied to winter conditions before.

Despite the extensive work published on quantifying the relative contributions of surface momentum flux to buoyancy flux in establishing the summer dynamics, there is no comparable work on the fall overturn period establishing the under-ice stratification. This idea has not been tested against a broad geographical suite of ice-covered lakes with differing depths, surface areas and wind speeds, likely because winter field work has substantial logistical challenges (Block et al., 2019). In this analysis, we use temperature and wind speed data from 19 lakes across North America, Europe, and Asia to explore the degree to which winter thermal stratification in ice-covered lakes is controlled by wind. Using these results, we suggest that the traditional classification by thermal regime and trophic status is not sufficient to understand the early winter stratification in dimictic lakes. We provide an additional classification for dimictic lakes based on the thermal stratification patterns across the different lakes in the study: *cryomictic* for lakes

that are cold and mixed at ice-on, and *cryostratified* for lakes that are warmer and stratified at ice-on. This additional classification has broad implications for our understanding of under-ice conditions in dimictic lakes.

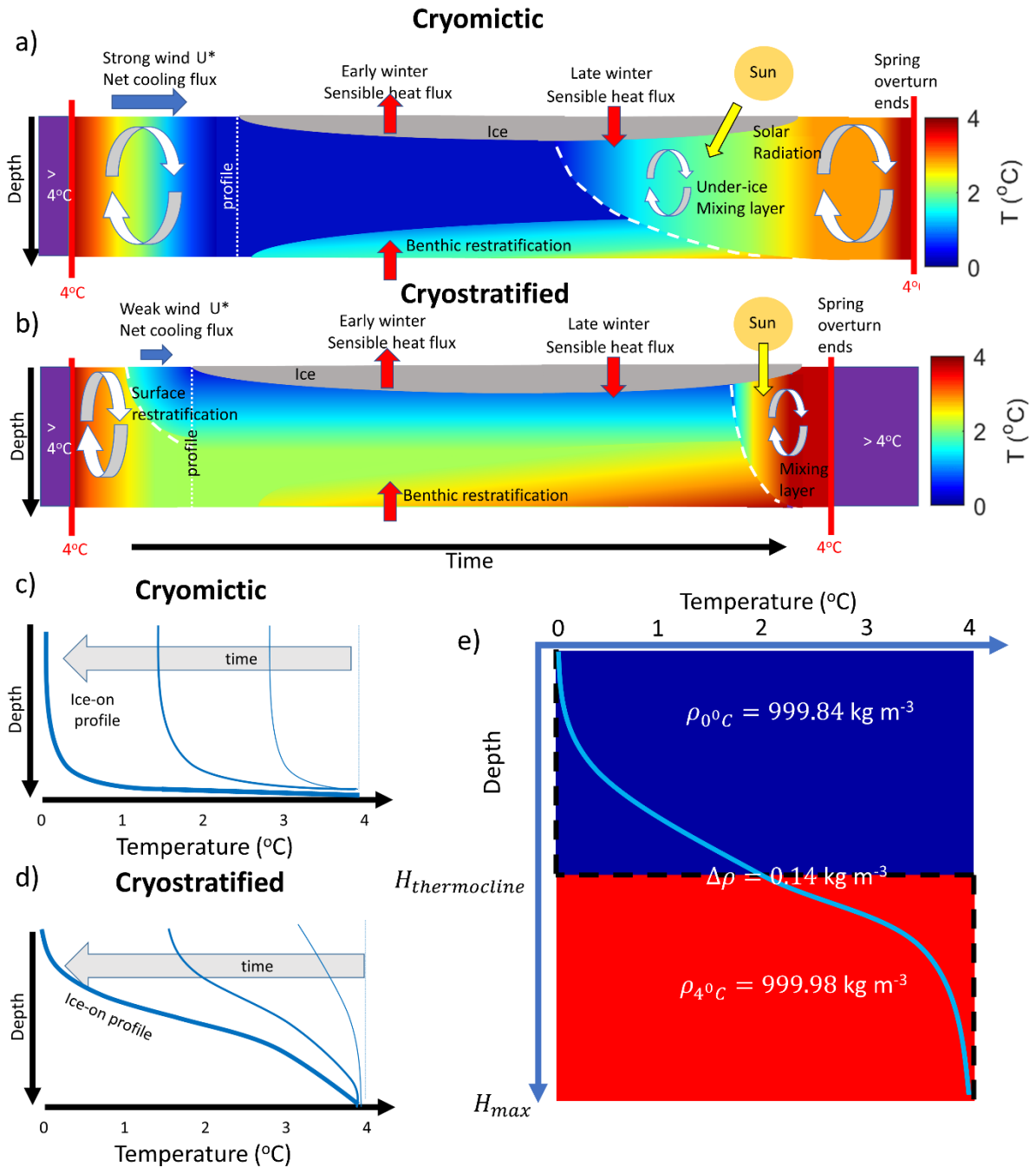


Figure 1: Schematic showing the difference in thermal structure between a) a wide, shallow, and windy lake with a deeper cold layer and weak stratification, and b) a small, deep, and calm lake with strong inverse stratification. Corresponding evolution of temperature profiles until ice-on

for c) wide lake and d) small lake. e) An idealized schematic of winter thermocline depth $H_{thermocline}$ used to develop our theory with the black dashed line showing the vertical temperature profile for the idealized two-layer model and the blue curve as an example of an actual vertical temperature profile.

Study Sites and Data

To analyze and classify the thermal profiles of lakes over a range of geographic locations with different climatic conditions, we used continuous water temperature measurements from 19 lakes across North America, Northern Europe, and Asia. This dataset covers a broad range of surface areas and maximum depths (Figure S1; Table S1). We defined the start of the inverse stratification period to be the time when the vertically averaged water temperature was 4°C, close to the temperature of maximum density of freshwater (Chen and Millero, 1986), and we defined the timing of ice-on to be the day of full ice cover. In larger lakes that are often partially ice-covered, we defined the timing of ice-on to be the first day where at least a radius of 10 km from the sampling point is ice-covered, which is consistent with the definition used in Titze and Austin (2016) (Table S1). In all lakes, water temperature was measured continuously at multiple depths (Table S1). The water temperature measurements were then extracted between the start of the inverse stratification period and the onset of ice-cover. Out of the 19 lakes in this study, 13 lakes included hourly wind speed measurements near the surface of the lake. Detailed lake characteristics including the geographic location, mean depth, maximum depth, surface area, and sampling rates are given in Table S1.

Calculating depth averaged temperatures

The depth-averaged temperature T_{avg} was calculated at the time of reported ice-on. In many cases moorings did not extend to the surface, due to vulnerability of the instruments to the lake ice, and instead the shallowest thermistors were typically below ice at 0.5 to 2-m depth. In these cases, we assumed that $T = 0$ at $z = 0$, and made a linear interpolation between that and the highest measurement. We also assumed that the temperature at the bottom was equal to the temperature at the deepest logger. Typically, this represents a slight underestimation of the actual depth-averaged temperature due to the inverse thermal stratification in cold lakes. However, there are special cases where compressibility effects were significant in very deep lakes (e.g. Lake Superior), resulting in an overestimation of the depth-averaged temperature at ice-on.

Calculating time averaged winds and the drag coefficient

For each lake, we determined the average surface wind at 10 m above the surface of the lake, U_{10} , by averaging the wind speeds between the start of inverse stratification and onset of ice cover. In cases where the wind measurements were made at another height z , we used a power-law scaling formula to estimate U_{10} following Hsu et al (1994).

$$U_{10} = U_z \left(\frac{10}{z} \right)^{0.11}$$

where U_z is the wind measured at height z above the surface of the lake. To account for the variability of the wind measurements during this period, we calculated the sample standard

deviation of all the wind speeds to obtain the wind speeds at the 25th and 75th percentile that were used to construct the error bars.

The drag coefficient $C_{D,10}$ was calculated using Charnock's Law (Charnock, 1955) and the empirical relationship determined by Wüest and Lorke (2003)

$$C_{D,10} = \begin{cases} 0.0044U_{10}^{-1.15}, & U_{10} < 5 \text{ m s}^{-1} \\ \left[\kappa^{-1} \ln \left(\frac{10g}{C_{D,10}U_{10}^2} \right) + 11.3 \right]^{-2}, & U_{10} > 5 \text{ m s}^{-1} \end{cases}$$

where κ is the von Karman constant and g is the gravitational acceleration.

Modelling Approach

Modelling the water temperature at ice formation based on wind measurements and geometry of the lake

The average temperature at ice-on can be estimated from a highly simplified two-layer model that has a top layer of thickness $H_{thermocline}$ and a total depth of H_{max} , where the temperature is set to 0°C above the winter thermocline and 4°C below (as sketched in Figure 1e). The depth averaged temperature of a lake at ice-on in degrees Celsius can be calculated as

$$T_{ice-on} = \frac{1}{H_{max}} (0 \times H_{thermocline} + 4 \times (H_{max} - H_{thermocline}))$$

which simplifies to

$$T_{avg} = 4 \left(1 - \frac{H_{thermocline}}{H_{max}} \right) \quad (2)$$

We define the depth of the thermocline based on the results of Gorham and Boyce (1989), who modelled the full scaling of the thermocline depth based on wind driven mixing events as

$$H_{thermocline} \equiv H_{GB} = 2 \left(\frac{\tau}{g\Delta\rho} \right)^{\frac{1}{2}} A^{\frac{1}{4}} \quad (3)$$

where τ is the surface wind stress, A is the surface area of the lake, and $\Delta\rho$ is the density difference between the two layers. The surface wind stress is given by

$$\tau \equiv \rho_w u_*^2 = \rho_a C_{D,10} U_{10}^2 \quad (4)$$

where ρ_w is the density of water (taken to be 1000 kg m⁻³ here), ρ_a is the density of air (1 kg m⁻³), U_{10} is the wind speed measured 10 m above the surface of the lake, and $C_{D,10}$ is the drag coefficient for surface winds at 10 m. Hence the friction velocity

$$u_* = \sqrt{\frac{\rho_A}{\rho_W} C_D U_{10}^2} \quad (5)$$

The local wind stress experienced between nearby lakes can vary (Read et al., 2012), depending upon local topography and the influence of wind sheltering (Markfort et al., 2010). Generally, these effects mean that larger lakes have stronger winds (i.e. $u_* \sim L$), when compared to nearby lakes of smaller area.

Combining equations 3–5, the depth of the thermocline can be written as

$$H_{thermocline} = 2 \left(\frac{\rho_a C_{D,10} U_{10}^2}{\rho_w g'} \right)^{\frac{1}{2}} A^{\frac{1}{4}} \quad (6)$$

where g' is the reduced gravity defined in terms of the density difference between 0 and 4°C water as $g' = g (\rho_{4^\circ\text{C}} - \rho_{0^\circ\text{C}}) / 0.5(\rho_{4^\circ\text{C}} + \rho_{0^\circ\text{C}})$. Using this, we obtain a novel estimation of the depth-averaged temperature at ice-on based on both the surface winds over the lake and the geometry of the lake by substituting into equation 1

$$\hat{T}_{ice-on} = \max \left\{ 0.4 \left(1 - \frac{2 \rho_a^{\frac{1}{2}} \rho_w^{-\frac{1}{2}} C_{D,10}^{\frac{1}{2}} g'^{-\frac{1}{2}} U_{10} A^{\frac{1}{4}}}{H_{max}} \right) \right\} = \max \left\{ 0.4 \left(1 - \frac{2 u_* g'^{-\frac{1}{2}} A^{\frac{1}{4}}}{H_{max}} \right) \right\} \quad (7)$$

Results

Detailed comparison of thermal stratification during the fall and winter between a small and large lake

Our new modelling approach suggests that local wind and lake area have important roles in determining the thermal profile at ice formation, and the extent to which dimictic lakes can vary between being cryomictic and cryostratified. This difference in thermal profiles is seen most clearly when comparing Lake Mendota (surface area 39.6 km²) with Harp Lake (surface area 0.714 km²). These lakes have similar maximum depths (25–30 m) and are at approximately the same latitude (43–45 degN) in mid-continental North America, thus experience relatively similar air temperatures and solar radiation. The most important difference between the lakes is the wind they experience. The average wind U_{10} on Lake Mendota at the start of the inverse stratification period and prior to ice-on was 5.8 m s⁻¹, much windier than the sheltered Harp Lake, where the average U_{10} was only 0.9 m s⁻¹ prior to ice formation. Consequently, temperature profiles of the two lakes at the time of initial ice formation were different, which influenced the stratification pattern during winter. During the early winter of 2019 between ice-on and February 1 in Lake Mendota, the water column was nearly isothermal. Before the surface-mixing layer started to develop in late March, most of the upper water column remained close to isothermal. Beneath the isothermal upper layer, the temperature was increasing at approximately 0.15°C m⁻¹, and the strongest stratification was at the bottom of the lake where the temperature increased at 0.5°C m⁻¹. In contrast, Harp Lake had only a thin surface layer near the surface that was less than 3°C. This surface layer was less than 3-m thick and strongly stratified where the maximum temperature

gradients were $1.5^{\circ}\text{C m}^{-1}$. Beneath this strongly stratified layer, the water column was between 3 and 4°C and the temperature gradients did not exceed $0.1^{\circ}\text{C m}^{-1}$.

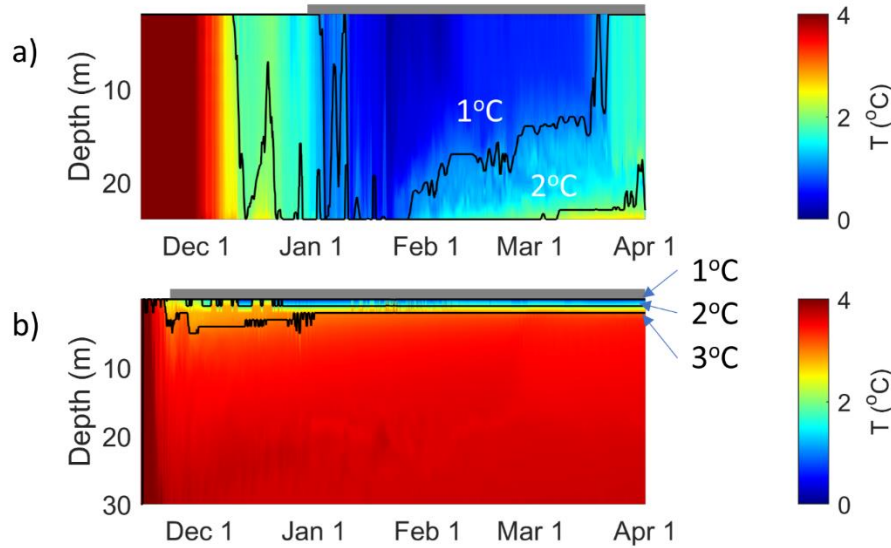


Figure 2: Difference in thermal structure between a) Lake Mendota (a large lake, 43.1°N), and b) Harp Lake (a small lake, 45.3°N) during the winter of 2019. These two lakes are at a similar latitude yet the thermal stratification in Lake Mendota was weak and colder compared to Harp Lake. While the Harp Lake site is 36-m deep, data are only shown for the top 30 m where continuous measurements were taken. In both plots, the gray bar on top of both plots indicate the duration of ice cover.

Comparison of water temperature at ice-on with lake size and the strength of surface winds

Extending the observations to 19 lakes globally, our data shows that the ice-on temperature profiles vary widely (Figure 3a). Lake Erie had the coldest temperature at ice-on at nearly 0°C and was nearly isothermal. The temperature profiles in other larger lakes such as Lake Simcoe were less than 1°C in the upper half of the water column, and between 1°C and 2°C near the bottom of the lake. In contrast, in other smaller lakes such as Alexie Lake, the water column was generally $> 2^{\circ}\text{C}$ where the temperature near the bottom can be close to 4°C , the temperature of maximum density.

We found a strong relationship between the surface winds and the depth-averaged ice-on temperatures. Lakes that experience weaker surface winds prior to ice-on had higher average temperatures at ice-on, while stronger winds led to lower average temperatures at ice-on (Figure 3b). This is consistent with stronger winds driving a deeper surface mixing layer prior to ice-on that transports colder waters to the bottom. The ice-on temperatures of each lake also appear to be well-correlated to the geometry of the lake H_{mean}/\sqrt{A} , where A is the surface area of the lake. This value is high for small, deep lakes and low for large, shallow lakes (Figure 3c). In general, we found that a larger surface area of the lake corresponds to higher average strength of the

surface winds (Figure 3d). The temperature scaling using our new idealized two-layer model (equation 7) agreed very well with the measured average temperature during ice-on (Figure 3e).

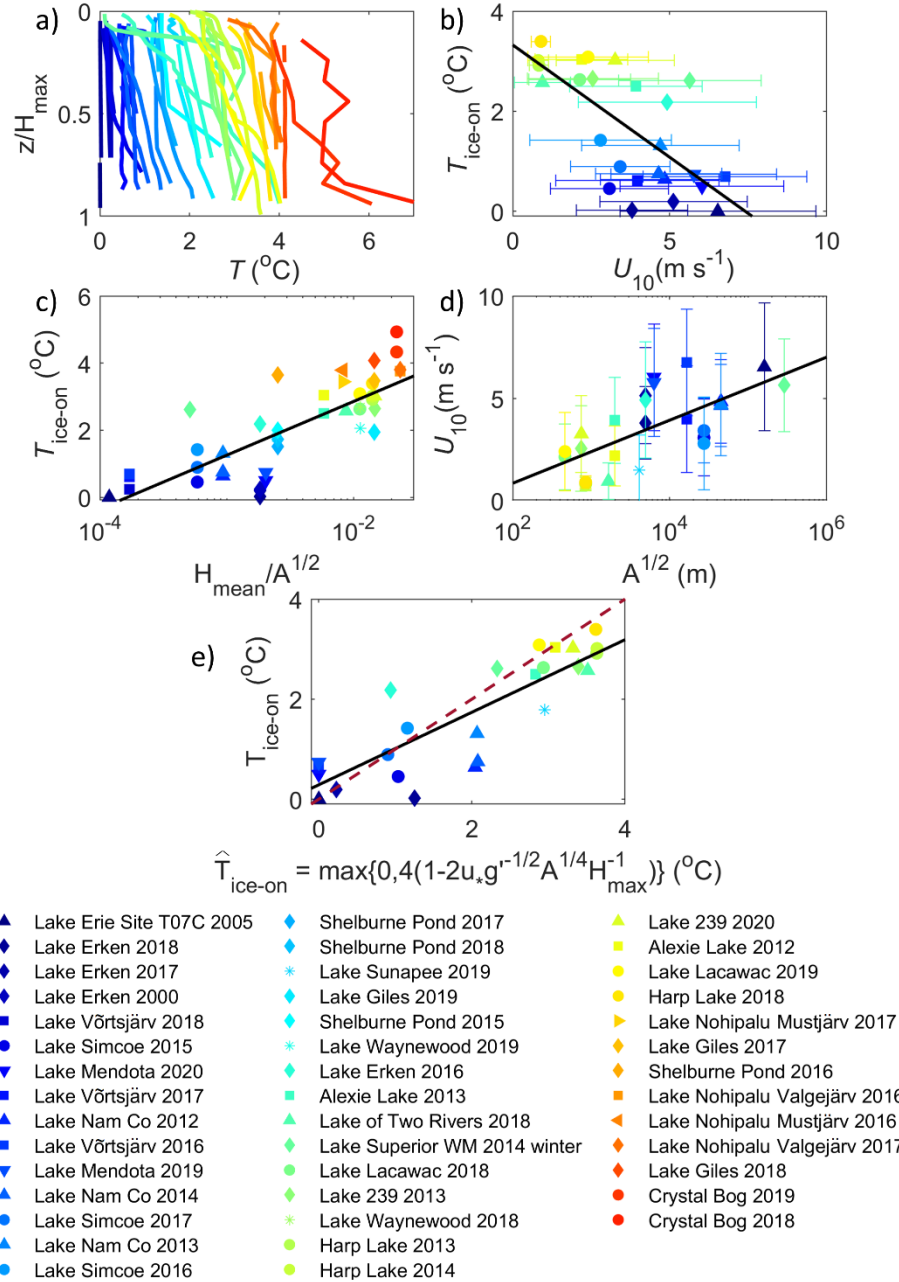


Figure 3: Water temperatures in our study lakes, each denoted by a unique color/symbol combination: a) Temperature profiles of each lake at ice-on with depth (z) on the y-axis normalized by the maximum depth of each lake (H_{\max}). b) Relationship between...Depth-averaged temperature at ice-on ($T_{\text{ice-on}}$) compared to $\overline{U_{10}}$, which, for lakes with wind data, was averaged from when the water column cooled to 4°C to ice-on. c) $T_{\text{ice-on}}$ compared to the ratio of the mean depth (H_{mean}) and the square root of the lake surface area ($A^{1/2}$). d) $\overline{U_{10}}$ during the same period in b) compared to $A^{1/2}$. e) Observed $T_{\text{ice-on}}$ compared to $\hat{T}_{\text{ice-on}}$ (modelled using

equation 7) with the dashed line representing 1:1. The black lines indicate the linear regressions for b) $T_{ice-on} = 3.32 - 0.45\bar{U}_{10}$, $R_{adj}^2 = 0.463$, slope $p < 0.01$, c) $T_{ice-on} = 6.32 + 0.73 \log(H_{mean}A^{-1/2})$, $R_{adj}^2 = 0.672$, slope $p < 0.0001$, d) $\bar{U}_{10} = -2.23 + 0.67 \log(A^{1/2})$, $R_{adj}^2 = 0.43$, slope $p < 0.001$, and e) $T_{ice-on} = 0.29 + 0.73 \hat{T}_{ice-on}$, $R_{adj}^2 = 0.726$, intercept $p = 0.177$, slope $p < 0.001$. Red colours indicate warmer T_{ice-on} and blue colours indicate colder T_{ice-on} .

Discussion

Our synthesis of data from 19 lakes in North America, Europe, and Asia suggests that there is a large variation of ice-on temperature profiles that vary between cryomictic and cryostratified, and that mean ice-on temperatures were well-predicted by lake depth, fetch and wind stress prior to ice-on (equation 7). For lakes without available wind data, we found that the depth-averaged temperature at ice-on correlated well with $\log(H_{mean}/\sqrt{A})$, where larger values indicate a deeper lake relative to its surface area. We emphasize that although the correlation coefficients R_{adj}^2 are similar between comparing T_{ice-on} against $\log(H_{mean}/\sqrt{A})$ ($R_{adj}^2 = 0.672$, Figure 3c) and comparing T_{ice-on} against the two-layer model scaling ($R_{adj}^2 = 0.726$, equation 7, Figure 3e), the new two-layer model scaling is based on the essential physics of the mixing layer depth proposed by Gorham and Boyce (1989) during wind events. However, if the friction velocity can be assumed to be an increasing function of \sqrt{A} (Figure 3d), then the two-layer model scaling (equation 7) suggests that T_{ice-on} will be a function of the vertical aspect ratio H_{mean}/\sqrt{A} (Figure 3c). Here, we found that most cryostratified lakes at ice-on have larger values of $\log(H_{mean}/\sqrt{A})$ and have weaker winds (Figure 3c).

More generally, the data and equation (7) suggest that the initial under-ice winter thermal stratification of a dimictic lake is best characterized by a gradient - on one end the depth-averaged temperatures are “cold” and close to 0°C with near uniform temperatures in a weakly stratified lake, whereas at the other end, the lake is “warm” with a thin cold layer of water immediately beneath the ice and then a deep layer of water that is near 4°C. In light of this, we suggest that it is useful to further subdivide the dimictic classification scheme of Lewis (1983) into additional categories and that the term “*inverse stratification*”, when applied widely to characterize seasonally ice-covered lakes, may be misleading in many cases. We suggest that a new term of “*cryostratified*” lakes be used when the depth-averaged initial winter temperature is between 2–4°C under the ice (i.e. Harp Lake, Figure 2b), and the term “*cryomictic*” lakes be used where depth-averaged temperatures are between 0–2 °C (i.e. Lake Mendota, Figure 2a). In the absence of additional chemical stratification, all initial under-ice winter temperature profiles exist on a continuum between these states. The use of these new will be helpful when comparing different lakes with regard to biogeochemical processes, fish habitat usage over winter, or advancing our understanding of under-ice dynamics in lakes. Here, we provide two examples of its relevance for biological and physical processes in lakes.

Implications of the new classification system for biological processes

The division of lakes into *cryostratified* and *cryomictic* may help to better understand the abundance of fish. Fish are ectotherms, so their use of different thermal habitat in a stratified water column has implications for their physiological rates and performance (Huey, 1991). Freshwater fish are known to select particular habitats that align with their thermal preferences (Brandt et al. 1980). However, much of this work has been restricted to open water periods. Fish habitat choice in winter, when temperatures range from near 0°C just below ice to temperatures as “warm” as 4°C at the bottom, is poorly understood. Both winter inactive (e.g. smallmouth bass, Suski and Ridgway, 2009) and winter active (e.g. burbot; Harrison et al., 2016) fish species appear to select for particular depths during winter, and a number of recent studies on salmonids suggest that these cold-adapted fish often occupy higher and colder regions of the water column in a narrow depth range during winter that corresponds to temperatures between 1–3°C (Blanchfield et al., 2009; McMeans et al., 2020; Bergstedt et al., 2003; Cote et al., 2020; Mulder et al., 2018; Gorsky et al., 2012). Although most ice-covered lakes have temperatures in the range 0–4°C, the degree of stratification can vary substantially between lakes. If fish are indeed choosing a specific 2°C isotherm, this layer would be deeper and potentially narrower in cryomictic lakes, versus cryostratified lakes. For instance, the 2°C isotherm is at approximately 90% of lake depth in the colder Lake Mendota, versus approximately 5% depth in Harp Lake (Figure 2). The degree to which differing winter stratification patterns drive different depth usage by various fish, and the resultant consequences for fish growth and survival, would therefore be a valuable research topic for future telemetry studies.

Implications of the new classification system for under-ice physical processes

Initial differences in thermal stratification under the ice influence late winter stratification, and can subsequently influence the magnitude of two key physical processes, namely (1) the duration and strength of vertical heat fluxes associated with the late winter radiatively driven convection, and (2) the timing and duration of spring overturn dynamics (Figure 1).

The duration and strength of late-winter convection depend on the buoyancy flux from solar radiation and the depth of the surface mixed layer. In cryostratified lakes, there is strong stratification so that there is a very thin surface mixed layer. In contrast, a small increase in under ice temperatures from solar heat can potentially trigger convective mixing throughout a large region of the water column in cold cryomictic lakes that are weakly stratified (Bruesewitz et al. 2015; Yang et al. 2017; Yang et al. 2020). In very large and deep lakes such as Lake Superior and Lake Michigan, the spring overturn can continue for weeks to months after ice-off, until the water column reaches 4°C (Austin, 2019; Cannon et al., 2019). Under similar meteorological forcing, we would expect that cryostratified lakes, such as Harp Lake (Figure 2b), will warm up to 4°C faster than colder cryomictic lakes after ice-off, and consequently have a shorter duration of spring overturn (Yang et al., 2020). We note that this is likely the reason that most previous studies on solar-driven convection have occurred in large deep lakes (Yang et al. 2017, 2020; Bouffard et al. 2019) rather than in smaller lakes that are typically warmer, and have only brief overturn periods (e.g. Bruesewitz et al. 2015). Similarly, the vertical velocities associated with solar-driven convection scale as $w^* \sim (Bh)^{\frac{1}{3}}$ (Kelley, 1997; Bouffard et al., 2019), where B is the buoyancy flux, and h is the depth of the surface mixed layer. It is likely that h is larger in cryomictic weakly stratified lakes during under-ice convection, and therefore these “colder” lakes are then more likely to have larger vertical velocities w^* and more vigorous convection

under the ice, as well as a longer duration of convection. The vigor of this convection may in turn structure the planktonic communities (Kelley, 1997; Bouffard et al., 2019) as plankton rely on the vertical circulation to remain in the photic zone (Yang et al., 2020).

Furthermore, both the data from 19 lakes (Figure 3e) and equation (7) suggest that the temperature at ice formation may be sensitive to shifts in surface winds. In particular, ice-on temperatures in larger lakes are more sensitive to differences in surface winds as equation (7) implies that $\left| \frac{\partial T_{avg}}{\partial u_*} \right| = 8g'^{\frac{1}{2}}A^{\frac{1}{4}}H_{max}^{-1}$ is greater for shallow lakes with larger area (see example in Figure S2). In some locations surface winds have increased by 10–20% recently (e.g. over Lake Superior, Desai et al., 2009), while in other locations winds have dropped by 10–20% (Pryor et al., 2009; Vautard et al., 2010). Such shifts in the mean surface winds or variability with late fall storm events on lakes that have ice-on temperatures that are close to 2°C might shift lakes between cryomictic and cryostratified states, depending on the surface winds.

Limitations of the analysis

The main assumption we have made in our analysis is that the thermal stratification at ice-on is primarily determined by surface heat fluxes and the turbulent mixing is driven by winds. Other processes could be important in setting winter thermal stratification. For example, river inflows can impact the thermal stratification (Pasche et al., 2019; Cortés and MacIntyre, 2019), which will be important in lakes that have short residence times. The summer heat stored in the sediment can also be an important heat flux (Fang and Stefan, 1996, 1998). Finally, in very deep lakes, such as Lake Superior, compressibility effects are important, so that stable temperature profiles below 200 m follow a thermobaric relationship, rather than being a constant 4°C (Titze and Austin, 2014; Crawford and Collier, 2007; Boehrer and Schultze, 2008). This implies that the depth averaged temperature of a deep lake at ice-on might be lower than expected based on similar shallow lakes.

Conclusions

Although Lewis (1983) originally classified all dimictic lakes into one group, we conclude that dimictic lakes should further be differentiated into *cryostratified* and *cryomictic*. We suggest that smaller lakes with less wind result in “warmer” under-ice temperatures near 4°C and should be termed “*cryostratified*” whereas larger lakes with higher winds are typically “colder” (near 0°C) and should be termed “*cryomictic*”. Stronger winds at the surface potentially drive a longer duration of mixing by delaying ice formation (Kirillin et al., 2012), and hence the temperature profiles at ice-on are colder and more isothermal compared to lakes with weaker winds. We developed an equation that predicts the mean temperature at ice-on from the wind speed and lake geometry (equation 7) and compares well with measurements from our study lakes. In cases where surface wind measurements are not available, the non-dimensional ratio $\log(H_{mean}/\sqrt{A})$ correlates well with the mean ice-on temperature. These results suggest that there is a wide spectrum of ice-on temperature profiles in temperate, dimictic lakes. Furthermore, we expect similar processes will occur in high latitude polymictic lakes or cold monomictic lakes. For example, Lake Vörtsjärv and Shelburne Pond were two polymictic lakes included in the analysis. greater recognition and better characterization of the variability in thermal structure under the ice

will have important implications for understanding both the ecology and physical dynamics of dimictic lakes during winter.

Data Availability Statement

References of all previously published data are available in Table S1 (Pierson et al. 2011; Cott et al. 2015; Guzzo et al. 2016; Titze and Austin 2016; Mackay et al. 2017; Yang et al. 2017; Moras et al. 2019; LSPA et al. 2020; McMeans et al. 2020; Wang et al. 2020; Yang et al. 2020). Previously unpublished data are available at <http://doi.org/10.5281/zenodo.4019639>.

Acknowledgements

We thank the Global Lake Ecological Observatory Network for organizing the GLEON 21 meeting, where this work was initially conceived. BY and MGW acknowledges support from the Ontario Ministry of Environment, Conservation, and Parks (Grant LS-14-15-011) and the NSERC Discovery program (Grant RGPIN-2016-06542). The Lake Superior observations were supported by National Science Foundation Division of Ocean Sciences grant OCE-0825633 and NSF RAPID (Grant OCE-1445567). AL acknowledges support from the Estonian Research Council Grant PSG32. GAW acknowledges the Swedish Infrastructure for Ecosystem Science (SITES) for provisioning of data from Lake Erken. SITES receives funding through the Swedish Research Council under the grant 2017-00635. Lake Mendota and Crystal Bog observations were supported by the US National Science Foundation grant DEB-1440297 and grant DEB-1856224. RMP acknowledges support from US National Science Foundation grants DEB 1754276 and DEB 1950170. CCC acknowledges support from US National Science Foundation grant DEB 1753639 and 1933016. Alexie Lake data collections were supported by DeBeers Canada and Fisheries & Oceans Canada

References

1. Austin, J. A. (2019). Observations of radiatively driven convection in a deep lake. *Limnology and Oceanography*, 64(5), 2152-2160. doi:
2. Bergstedt, R. A., Argyle, R. L., Seelye, J. G., Scribner, K. T., & Curtis, G. L. (2003). In situ determination of the annual thermal habitat use by lake trout (*Salvelinus namaycush*) in Lake Huron. *Journal of Great Lakes Research*, 29, 347-361. doi:10.1016/S0380-1330(03)70499-7
3. Blanchfield, P. J., Tate, L. S., Plumb, J. M., Acolas, M. L., & Beaty, K. G. (2009). Seasonal habitat selection by lake trout (*Salvelinus namaycush*) in a small Canadian shield lake: constraints imposed by winter conditions. *Aquatic ecology*, 43(3), 777-787. doi: 10.1007/s10452-009-9266-3

4. Block, B. D., Denfeld, B. A., Stockwell, J. D., Flaim, G., Grossart, H. P. F., Knoll, L. B.,
... & Sadro, S. (2019). The unique methodological challenges of winter
limnology. *Limnology and Oceanography: Methods*, 17(1), 42-57.
doi:10.1002/lom3.10295
5. Boehrer, B., & Schultze, M. (2008). Stratification of lakes. *Reviews of Geophysics*, 46(2).
doi: 10.1029/2006RG000210
6. Bouffard, D., Zdrovennova, G., Bogdanov, S., Efremova, T., Lavanchy, S., Palshin, N.,
... & Zdrovennov, R. (2019). Under-ice convection dynamics in a boreal lake. *Inland
Waters*, 9(2), 142-161. doi:10.1080/20442041.2018.1533356
7. Brandt, S. B., Magnuson, J. J., & Crowder, L. B. (1980). Thermal habitat partitioning by
fishes in Lake Michigan. *Canadian Journal of Fisheries and Aquatic Sciences*, 37(10),
1557-1564.
8. Bruesewitz, D. A., Carey, C. C., Richardson, D. C., & Weathers, K. C. (2015). Under-ice
thermal stratification dynamics of a large, deep lake revealed by high-frequency
data. *Limnology and Oceanography*, 60(2), 347-359. doi: 10.1005/lno.10014
9. Cannon, D. J., Troy, C. D., Liao, Q., & Bootsma, H. A. (2019). Ice-free radiative
convection drives spring mixing in a large lake. *Geophysical Research Letters*, 46(12),
6811-6820. doi: 10.1029/2019GL082916
10. Charnock, H. (1955). Wind stress on a water surface. *Quarterly Journal of the Royal
Meteorological Society*, 81(350), 639-640. doi: 10.1002/qj.49708135027
11. Chen, C. T. A., & Millero, F. J. (1986). Thermodynamic properties for natural waters
covering only the limnological range. *Limnology and Oceanography*, 31(3), 657-662.
doi: 10.4319/lo.1986.31.3.0657
12. Cortés, A., & MacIntyre, S. (2019). Mixing processes in small arctic lakes during
spring. *Limnology and Oceanography*. doi: 10.1002/lno.11296
13. Cote, D., Tibble, B., Curry, R. A., Peake, S., Adams, B. K., Clarke, K. D., & Perry, R.
(2020). Seasonal and diel patterns in activity and habitat use by brook trout (*Salvelinus
fontinalis*) in a small Newfoundland lake. *Environmental Biology of Fishes*, 103(1), 31-
47. doi: 10.1007/s10641-019-00931-1
14. Cott, P. A., Guzzo, M. M., Chapelsky, A. J., Milne, S. W., & Blanchfield, P. J. (2015).
Diel bank migration of Burbot (*Lota lota*). *Hydrobiologia*, 757(1), 3-20. doi:
10.1007/s10750-015-2257-6

- 574 15. Crawford, G. B., & Collier, R. W. (2007). Long-term observations of deepwater renewal
575 in Crater Lake, Oregon. *Hydrobiologia*, 574(1), 47-68. doi: 10.1007/s10750-006-0345-3
- 576 16. Crossin, G. T., Heupel, M. R., Holbrook, C. M., Hussey, N. E., Lowerre-Barbieri, S. K.,
577 Nguyen, V. M., ... & Cooke, S. J. (2017). Acoustic telemetry and fisheries
578 management. *Ecological Applications*, 27(4), 1031-1049. doi: 10.1002/eap.1533
- 579 17. Desai, A. R., Austin, J. A., Bennington, V., & McKinley, G. A. (2009). Stronger winds
580 over a large lake in response to weakening air-to-lake temperature gradient. *Nature*
581 *Geoscience*, 2(12), 855-858. doi: 10.1038/ngeo693
- 582 18. Fang, X., & Stefan, H. G. (1996). Dynamics of heat exchange between sediment and
583 water in a lake. *Water Resources Research*, 32(6), 1719-1727. doi: 10.1029/96WR00274
- 584 19. Fang, X., & Stefan, H. G. (1998). Temperature variability in lake sediments. *Water*
585 *Resources Research*, 34(4), 717-729. doi: 10.1029/97WR03517
- 586 20. Fee, E. J., Hecky, R. E., Kasian, S. E. M., & Cruikshank, D. R. (1996). Effects of lake
587 size, water clarity, and climatic variability on mixing depths in Canadian Shield
588 lakes. *Limnology and Oceanography*, 41(5), 912-920. doi: 10.4319/lo.1996.41.5.0912
- 589 21. Farmer, D. M., & Carmack, E. (1981). Wind mixing and restratification in a lake near the
590 temperature of maximum density. *Journal of physical oceanography*, 11(11), 1516-1533.
591 doi: 10.1175/1520-0485(1981)011<1516:WMARIA>2.0.CO;2
- 592 22. Gorham, E., & Boyce, F. M. (1989). Influence of lake surface area and depth upon
593 thermal stratification and the depth of the summer thermocline. *Journal of Great Lakes*
594 *Research*, 15(2), 233-245. doi: 10.1016/S0380-1330(89)71479-9
- 595 23. Gorsky, D., Zydlewski, J., & Basley, D. (2012). Characterizing seasonal habitat use and
596 diel vertical activity of lake whitefish in Clear Lake, Maine, as determined with acoustic
597 telemetry. *Transactions of the American Fisheries Society*, 141(3), 761-771.
598 doi:10.1080/00028487.2012.675905
- 599 24. Guseva, S., Bleninger, T., Jöhnk, K., Polli, B. A., Tan, Z., Thiery, W., ... & Stepanenko,
600 V. (2020). Multimodel simulation of vertical gas transfer in a temperate lake. *Hydrology*
601 *and Earth System Sciences*, 24(2), 697-715. doi: 10.5194/hess-24-697-2020
- 602 25. Guzzo, M. M., Blanchfield, P. J., Chapelsky, A. J., & Cott, P. A. (2016). Resource
603 partitioning among top-level piscivores in a sub-Arctic lake during thermal
604 stratification. *Journal of Great Lakes Research*, 42(2), 276-285. doi:
605 10.1016/j.jglr.2015.05.014

26. Hampton, S. E., Galloway, A. W., Powers, S. M., Ozersky, T., Woo, K. H., Batt, R. D., ...
& Stanley, E. H. (2017). Ecology under lake ice. *Ecology letters*, 20(1), 98-111. doi:
10.1111/ele.12699
27. Hampton, S. E., Moore, M. V., Ozersky, T., Stanley, E. H., Polashenski, C. M., &
Galloway, A. W. (2015). Heating up a cold subject: prospects for under-ice plankton
research in lakes. *Journal of plankton research*, 37(2), 277-284. doi:
10.1093/plankt/fbv002
28. Harrison, P. M., Gutowsky, L. F. G., Martins, E. G., Patterson, D. A., Cooke, S. J., &
Power, M. (2016). Temporal plasticity in thermal-habitat selection of burbot *Lota lota* a
diel-migrating winter-specialist. *Journal of Fish Biology*, 88(6), 2111-2129. doi:
10.1111/jfb.12990
29. Huey, R. B. (1991). Physiological consequences of habitat selection. *The American
Naturalist*, 137, S91-S115. doi: 10.1086/285141
30. Hsu, S. A., Meindl, E. A., & Gilhousen, D. B. (1994). Determining the power-law wind-
profile exponent under near-neutral stability conditions at sea. *Journal of Applied
Meteorology*, 33(6), 757-765. doi: 10.1175/1520-
0450(1994)033<0757:DTPLWP>2.0.CO;2
31. Kelley, D. E. (1997). Convection in ice-covered lakes: effects on algal
suspension. *Journal of Plankton Research*, 19(12), 1859-1880. doi:
10.1093/plankt/19.12.1859
32. Kirillin, G., & Shatwell, T. (2016). Generalized scaling of seasonal thermal stratification
in lakes. *Earth-Science Reviews*, 161, 179-190. doi: 10.1016/j.earscirev.2016.08.008
33. Kirillin, G., Leppäranta, M., Terzhevik, A., Granin, N., Bernhardt, J., Engelhardt, C., ...
& Zdrovennova, G. (2012). Physics of seasonally ice-covered lakes: a review. *Aquatic
sciences*, 74(4), 659-682. doi: 10.1007/s00027-012-0279-y
34. Lewis Jr, W. M. (1983). A revised classification of lakes based on mixing. *Canadian
Journal of Fisheries and Aquatic Sciences*, 40(10), 1779-1787. doi: 10.1139/f83-207
35. LSPA, K.C. Weathers, and B.G. Steele. 2020. High-Frequency Weather Data at Lake
Sunapee, New Hampshire, USA, 2007-2019 ver 3. Environmental Data Initiative. Doi:
10.6073/pasta/698e9ffb0cdcd81ecf7188bff54445e. Accessed 2020-05-14

36. MacKay, M. D., Versegny, D. L., Fortin, V., & Rennie, M. D. (2017). Wintertime simulations of a boreal lake with the Canadian Small Lake Model. *Journal of Hydrometeorology*, 18(8), 2143-2160. doi: 10.1175/JHM-D-16-0268.1
37. Markfort, C. D., Perez, A. L., Thill, J. W., Jaster, D. A., Porté-Agel, F., & Stefan, H. G. (2010). Wind sheltering of a lake by a tree canopy or bluff topography. *Water Resources Research*, 46(3). doi: 10.1029/2009WR007759
38. McMeans, B. C., McCann, K. S., Guzzo, M. M., Bartley, T. J., Bieg, C., Blanchfield, P. J., ... & Ridgway, M. S. (2020). Winter in water: Differential responses and the maintenance of biodiversity. *Ecology Letters*, 23(6), 922-938. doi: 10.1111/ele.13504
39. Moras, S., Ayala, A. I., & Pierson, D. (2019). Historical modelling of changes in Lake Erken thermal conditions. *Hydrology and Earth System Sciences*, 23(12), 5001-5016. doi: 10.5194/hess-23-5001-2019
40. Mulder, I. M., Morris, C. J., Dempson, J. B., Fleming, I. A., & Power, M. (2018). Overwinter thermal habitat use in lakes by anadromous Arctic char. *Canadian Journal of Fisheries and Aquatic Sciences*, 75(12), 2343-2353. doi: 10.1139/cjfas-2017-0420
41. O'Reilly, C. M., Sharma, S., Gray, D. K., Hampton, S. E., Read, J. S., Rowley, R. J., ... & Weyhenmeyer, G. A. (2015). Rapid and highly variable warming of lake surface waters around the globe. *Geophysical Research Letters*, 42(24), 10773-10781. doi: 10.1002/2015GL066235
42. Pasche, N., Hofmann, H., Bouffard, D., Schubert, C. J., Lozovik, P. A., & Sobek, S. (2019). Implications of river intrusion and convective mixing on the spatial and temporal variability of under-ice CO₂. *Inland Waters*, 9(2), 162-176. doi: 10.1080/20442041.2019.1568073
43. Pierson, D. C., Weyhenmeyer, G. A., Arvola, L., Benson, B., Blenckner, T., Kratz, T., ... & Weathers, K. (2011). An automated method to monitor lake ice phenology. *Limnology and Oceanography: Methods*, 9(2), 74-83. doi: 10.4319/lom.2010.9.0074
44. Pryor, S. C., Barthelmie, R. J., Young, D. T., Takle, E. S., Arritt, R. W., Flory, D., ... & Roads, J. (2009). Wind speed trends over the contiguous United States. *Journal of Geophysical Research: Atmospheres*, 114(D14). doi: 10.1029/2008JD011416

45. Read, J. S., Hamilton, D. P., Desai, A. R., Rose, K. C., MacIntyre, S., Lenters, J. D., ... & Rusak, J. A. (2012). Lake-size dependency of wind shear and convection as controls on gas exchange. *Geophysical Research Letters*, 39(9). doi: 10.1029/2012GL051886
46. Suski, C. D., & Ridgway, M. S. (2009). Seasonal pattern of depth selection in smallmouth bass. *Journal of Zoology*, 279(2), 119-128. doi: 10.1111/j.1469-7998.2009.00595.x
47. Titze, D. J., & Austin, J. A. (2014). Winter thermal structure of Lake Superior. *Limnology and oceanography*, 59(4), 1336-1348. doi: 10.4319/lo.2014.59.4.1336
48. Titze, D., & Austin, J. (2016). Novel, direct observations of ice on Lake Superior during the high ice coverage of winter 2013–2014. *Journal of Great Lakes Research*, 42(5), 997-1006. doi: 10.1016/j.jglr.2016.07.026
49. Wang, J., Huang, L., Ju, J., Daut, G., Ma, Q., Zhu, L., ... & Graves, K. (2020). Seasonal stratification of a deep, high-altitude, dimictic lake: Nam Co, Tibetan Plateau. *Journal of Hydrology*, 584, 124668. doi: 10.1016/j.jhydrol.2020.124668
50. Wüest, A., & Lorke, A. (2003). Small-scale hydrodynamics in lakes. *Annual Review of fluid mechanics*, 35(1), 373-412. doi: 10.1146/annurev.fluid.35.101101.161220
51. Vautard, R., Cattiaux, J., Yiou, P., Thépaut, J. N., & Ciais, P. (2010). Northern Hemisphere atmospheric stilling partly attributed to an increase in surface roughness. *Nature geoscience*, 3(11), 756-761. doi: 10.1038/ngeo979
52. Verpoorter, C., Kutser, T., Seekell, D. A., & Tranvik, L. J. (2014). A global inventory of lakes based on high-resolution satellite imagery. *Geophysical Research Letters*, 41(18), 6396-6402. doi: 10.1002/2014GL060641
53. Wetzel, R. G. (2001). *Limnology: lake and river ecosystems*. gulf professional publishing.
54. Yang, B., Young, J., Brown, L., & Wells, M. (2017). High-frequency observations of temperature and dissolved oxygen reveal under-ice convection in a large lake. *Geophysical Research Letters*, 44(24), 12218-12226. doi: 10.1002/2017GL075373
55. Yang, B., Wells, M. G., Li, J., & Young, J. (2020). Mixing, stratification, and plankton under lake-ice during winter in a large lake: Implications for spring dissolved oxygen levels. *Limnology and Oceanography*. doi: 10.1002/lno.11543

